Performance of the TALE infill experiment as a TA-TALE extension down to the PeV region

Aoi Iwasaki[1,*], *Keitaro* Fujita, *Shoichi* Ogio, *Toshihiro* Fujii, and *Yoshiki* Tsunesada for the Telescope Array Collaboration

[1]Osaka Metropolitan University
[2]University of Tokyo

Abstract. The TALE infill experiment is a further extension of TA-TALE detectors to observe low-energy cosmic rays down to the PeV region. TALE infill utilizes the existing TALE-FD detectors, and newly developed "infill" surface detectors with 100 m and 200 m spacing. The new detectors will be deployed at the TALE site in October-November 2022. We present the design and performance of the TALE infill array in the hybrid mode, in terms of the resolutions and biases of arrival direction, energy, and $X_{\max}$.

1 TALE infill : Science goals

This is the first experiment in the world to observe low-energy cosmic rays using both a Surface Detector (SD) and Fluorescence Detector (FD). By using TALE infill hybrid, we want to accurately measure mass composition in the low energy range, where results vary from experiment to experiment(Fig.1), and unravel the knee structure which is thought to be the energy range where cosmic rays transition from lighter nuclei to heavier nuclei. Therefore, it is necessary to distinguish at least protons and iron in the PeV region.

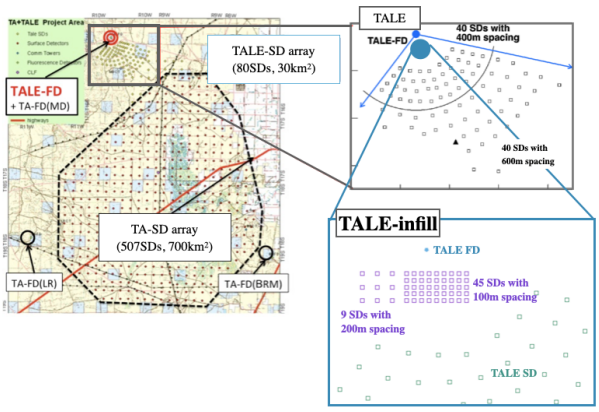

Figure 2: The layout of the TA detector, the TALE detector, and the TALE infill detector. TALE infill SDs, represented by purple square, are located between TALE-FD and TALE-SDs.

2 Detectors

2.1 TALE infill SD array

The TALE-SDs are located northwest of the TA-SDs. To observe cosmic rays with energies lower than the TALE experiment, the TALE infill SDs are deployed closer to the TALE-FD and denser than the TALE-SDs. TALE infill SDs have 100 m spacing area and 200 m spacing area. By creating a high density area, it's possible to observe low energy CRs. By creating a low density area, it's possible to eliminate energy gap between the TALE hybrid experiment.

2.2 Hybrid observation

FD observes the air fluorescence and cherenkov photons to determine the longitudinal development of air showers. Since September 2013, TALE-FD has been operational with 10 telescopes. TALE-FD station has a field of view from 30° to 57° in the Elevation direction and 114° in the azimuth direction. On the other hand, SD measures the lateral distribution of air shower charged particles. TALE-infill SD was created in October 2021. We will deploy that in October-November 2022. By using both information on longitudinal and ground, the hybrid observation has better resolution than other observation methods.

*e-mail: m21sa004@st.osaka-cu.ac.jp

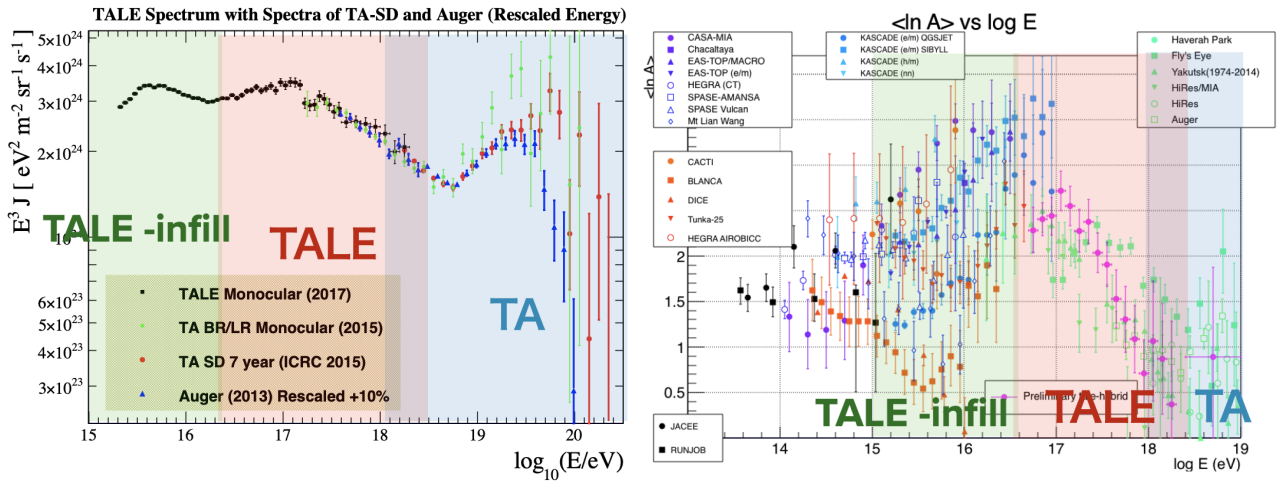

Figure 1: Energy spectrum (left) and composition (right) from the knee region onwards. Measurements of $\langle X_{\max} \rangle$ with direct observation(JACEE [1], RUNJOB [2]) are shown in black. Experiments using chamber light obesrvation(CACTI [3], BALANCA [4], DICE [5], Tunka-25 [6], HEGRA AIROBICC [7]) are shown in orange. Purple represents $\langle X_{\max} \rangle$ by the experiments observing around the knee range(CASA_MIA [8], Chacaltaya [9], EAS_TOPMACRO [10], EAS_TOP(em) [11], HEGRA(CT) [12], SPASE_AMANSA [13], SPASE Vulcan [14], Mt Lian Wang [15]), and light blue represents $\langle X_{\max} \rangle$ by the KASCADE experiment group(KASCADE(em) QGSJET [16], KASCADE (em) SIBYLL [16], KASCADE(hm) [17], KASCADE(nn) [18]), green represents $\langle X_{\max} \rangle$ by the experiments observing ultra high energy range(Haverah Park [19], Fly's Eye [20], Yakutsk [21], HiResMIA [22], HiRes [23], Auger [24]), and pink represents $\langle X_{\max} \rangle$ by the TA hybrid. The blue, red and green regions represent the observed energies of the TA, TALE, and TALE infill experiments respectively.

(a) The Fluorescence Detector (FD).

(b) The Surface Detector (SD).

Figure 3: (a) : The Middle Drum station for TA experiment is on the left, and the TALE-FD station on the right. (b) : The scintillator under the brown iron observes the charged particles.

3 Simulation

We simulated air showers by the CORSIKA for proton and iron primaries. The energy is $10^{15.2}$ eV, $10^{15.4}$ eV, $10^{15.6}$ eV, $10^{15.8}$ eV, $10^{16.0}$ eV, $10^{16.2}$ eV and $10^{16.5}$ eV (fixed for each energy). Zenith angle and Azimuthal angle ranges are 0° to 60° and 0° to 360° with uniformly random distributions, respectively. The core position is uniformly random distributed within a semi-circle of 1.4 km radius shown in Fig.4. All of the calibration factors with time dependence are applied to SD and FD detector simulations.

We select events that satisfy the quality cuts conditions in Table.1 from those that pass reconstruction, in order to remove poorly reconstructed events and ensure good detector resolution. We define fluorescence events as fractional contribution to the total signal of Fluorescence Light (FL) > 0.75, and Cherenkov events as fractional contribution to the total signal of FL ≦ 0.75.

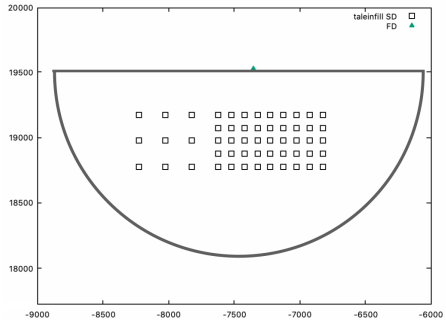

Figure 4: Core location distribution of Monte Carlo showers.

4 Event distribution @$10^{16.0}$ eV

An example of event distribution that passed reconstruction are shown in Fig.5. The reason for the small number of events with azimuths of 150° is that the shutters of the FD stations viewing this angle were closed at the time of the simulation.

Variable	CL	FL
No saturated PMTs in FD	applied	
SD detected ≥ 3 MIPs	applied	
X_{max} in TALE-FD viewing angle	applied	
Angular track-length [deg]	$> 8°$	-
Event duration [μs]	$> 0.1\,\mu$s	-
# of PMTs	> 10	-
# of Photo-electrons / # of PMTs	> 50	-
# of Photo-electrons	-	> 2000

Table 1: quality cuts applied in this study.

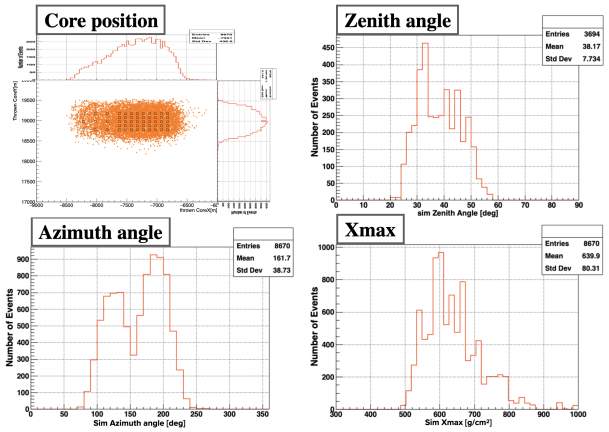

Figure 5: The event distribution of core position (upper left), zenith angle (upper right), azimuth angle (lower left), and X_{max} (lower right).

5 Parameter resolution

The resolution of X_{max} and Energy are shown in Fig.6.

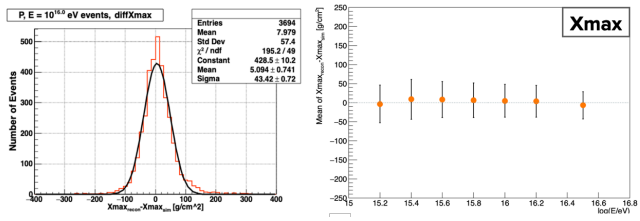

(a) The resolution of X_{max} ($5.1 \pm 43.4\,\mathrm{g/cm^2}$ at $10^{16.0}$ eV).

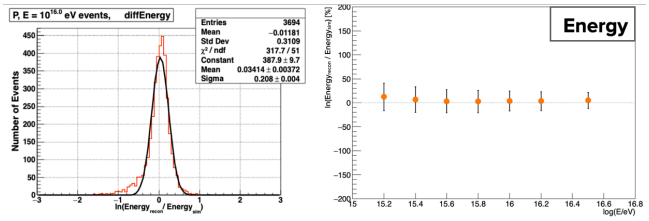

(b) The resolution of Energy(3.4 ± 20.8 % at $10^{16.0}$ eV).

Figure 6: The resolution of parameter. The plots and error bars on the right are the mean and sigma obtained by figging the histogram on the left with the Gaussian function.

6 Mean X_{max} bias

Fig.7 shows thrown $\langle X_{max}^{true} \rangle$ without any reconstructions, triggered $\langle X_{max}^{true} \rangle$, reconstructed $\langle X_{max}^{true} \rangle$, and reconstructed $\left\langle X_{max}^{reconstructed} \right\rangle$ with quality cuts using TALE infill hybrid. The $\langle X_{max} \rangle$ bias is estimated from difference between thrown $\langle X_{max}^{true} \rangle$ and reconstructed $\left\langle X_{max}^{reconstructed} \right\rangle$ with quality cuts.The maximum value of the bias os $50\,\mathrm{g/cm^2}$. The mass composition measurement of CRs at the knee region has been validated from this simulation studies.

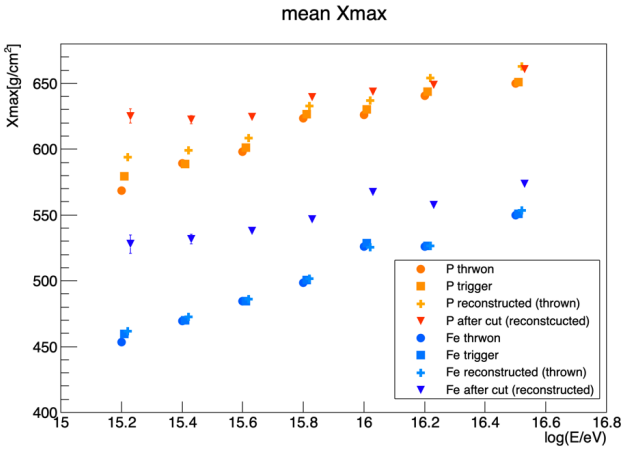

Figure 7: The $\langle X_{max} \rangle$ bias for proton (orange) and iron(blue). These points represent thrown $\langle X_{max}^{true} \rangle$ (circle), triggered $\langle X_{max}^{true} \rangle$ (square), reconstructed $\langle X_{max}^{true} \rangle$ (plus), and reconstructed $\left\langle X_{max}^{reconstructed} \right\rangle$ with quality cuts (inverse triangle).

7 Future work

Considering the bias of the parameter resolution and mean X_{max}, the X_{max} resolution is better than $40\,\mathrm{g/cm^2}$ by optimizing the quality cuts.

acknowledgements

The TALE SD production and the TALE hybrid operations are supported by the Japan Society for the Promotion of Science(JSPS) through Grants-in-Aid for Scientific Research (S) 15H05741 and 19H05607; by the joint research program of the Institute for Cosmic Ray Research (ICRR), The University of Tokyo. The experimental site became available through the cooperation of the Utah School and Institutional Trust Lands Administration (SITLA), U.S. Bureau of Land Management (BLM), and the U.S. Air Force. We appreciate the assistance of the State of Utah and Fillmore offices of the BLM in crafting the Plan of Development for the site. The people and the officials of Millard County, Utah have been a source of steadfast and warm support for our work which we greatly appreciate. We gratefully acknowledge the contribution from the technical staffs of our home institutions.

References

[1] Y. Takahashi, Nuclear Physics B - Proceedings Supplements **60**, 83 (1998)

[2] V.A. Derbina et al. (RUNJOB), Astrophys. J. Lett. **628**, L41 (2005)

[3] S. Paling et al., ,, in *25th International Cosmic Ray Conference* (1997), p. 253

[4] J.W. Fowler, L.F. Fortson, C.C.H. Jui, D.B. Kieda, R.A. Ong, C.L. Pryke, P. Sommers, Astropart. Phys. **15**, 49 (2001), astro-ph/0003190

[5] S.P. Swordy, D.B. Kieda, Astropart. Phys. **13**, 137 (2000), astro-ph/9909381

[6] D. Chernov et al., Int. J. Mod. Phys. A **20**, 6799 (2006), astro-ph/0411139

[7] F. Arqueros et al. (HEGRA), Astron. Astrophys. **359**, 682 (2000), astro-ph/9908202

[8] M.A.K. Glasmacher et al., *"The cosmic ray energy spectrum from* 10^{14} eV *to* 10^{16} eV*,"*, in *26th International Cosmic Ray Conference* (1999)

[9] C. Aguirre et al., Phys. Rev. D **62**, 032003 (2000)

[10] C. Aguirre, H. Aoki, K. Hashimoto, K. Honda, N. Inoue, N. Kawasumi, Y. Maeda, N. Martinic, T. Matano, N. Ohmori et al., Phys. Rev. D **62**, 032003 (2000)

[11] M. Aglietta et al. (EAS-TOP), Astropart. Phys. **21**, 583 (2004)

[12] K. Bernlohr, W. Hofmann, G. Leffers, V. Matheis, M. Panter, R. Zink, Astropart. Phys. **8**, 253 (1998), astro-ph/9801042

[13] K. Rawlins (SPASE, AMANDA), *"Measurement of the cosmic ray composition at the knee with the SPASE-2/AMANDA-B10 detectors,"*, in *28th International Cosmic Ray Conference* (2003), pp. 173–176

[14] J.E. Dickinson et al., *"Studies of the mass composition of cosmic rays with the SPASE-2/VULCAN instrument at the South Pole,"*, in *26th International Cosmic Ray Conference* (1999)

[15] M. Cha et al., ,, in *27th International Cosmic Ray Conference* (2001), p. 132

[16] T. Antoni et al. (KASCADE), Astropart. Phys. **24**, 1 (2005), astro-ph/0505413

[17] J. Horandel et al., in *16th European Cosmic Ray Symposium* (1998), p. 579

[18] T. Antoni et al. (KASCADE), Astropart. Phys. **16**, 245 (2002), astro-ph/0102443

[19] M. Ave, L. Cazon, J.A. Hinton, J. Knapp, J. LLoyd-Evans, A.A. Watson, Astropart. Phys. **19**, 61 (2003), astro-ph/0203150

[20] D.J. Bird et al. (HiRes), Astrophys. J. **424**, 491 (1994)

[21] S.P. Knurenko, A.A. Ivanov, A.V. Sabourov, I.Y. Sleptsov, *"Average Mass Composition of Primary Cosmic Rays in the Superhigh Energy Region by the Yakutsk Complex EAS Array Data,"*, in *30th International Cosmic Ray Conference* (2007), Vol. 4, pp. 167–170, 0711.2348

[22] T. Abu-Zayyad et al. (HiRes-MIA), Astrophys. J. **557**, 686 (2001), astro-ph/0010652

[23] R.U. Abbasi et al. (HiRes), Astrophys. J. **622**, 910 (2005), astro-ph/0407622

[24] M. Unger (Pierre Auger), Astron. Nachr. **328**, 614 (2007), 0706.1495